

Friction and Wear of Aluminum Alloy Reinforced by TiO₂ Particles

Z. Sarajan

Islamic Azad University, Yazd, Iran

zohairsarajan@yahoo.com

УДК 539.4

Трение и износ алюминиевого сплава, упрочненного частицами TiO₂

З. Сараян

Исламский университет Азад Йезд, Йезд, Иран

Исследуемый композит получен путем добавления от 0,5 до 3,5 мас.% порошка TiO₂ в алюминиевый расплав по технологии так называемой обработки полужатвердевшего металла, используемой для получения алюминиевых сплавов. Литой композит, полученный путем кристаллизации расплава с частицами TiO₂ в форме, испытывали на износ при сухом трении по трибосхеме диск-шпилька. Испытания проводили без удаления продуктов износа согласно стандартной схеме и с удалением таковых с помощью волосяной кисточки. Объемный износ композита линейно возрастает с увеличением длины скольжения, а скорость износа возрастает более-менее линейно с повышением нагрузки. С увеличением содержания частиц TiO₂ уменьшается скорость износа при заданной нагрузке. Объемный износ композита оказывается значительно выше, если продукты износа удаляются в процессе сухого трения. На электронных микрографиях изношенных контактных поверхностей композитов, полученных путем добавления порошка TiO₂, можно наблюдать ярко выраженный уплотненный переходный оксидный слой. При более высоких нагрузках оксидные продукты износа предположительно уменьшаются и образуют прослойку, которая распространяется на большую площадь поверхности скольжения. Таким образом, удаление оксидных продуктов износа приводит к большему износу композита по сравнению с испытаниями без удаления.

Ключевые слова: процесс полужатвердения, порошок TiO₂, композит, износ при сухом скольжении, переходной слой.

Introduction. Over the last two decades, a lot of research has been focused on aluminum metal matrix composites (Al MMCs). A wide variety of fabrication techniques have been explored for Al MMCs, which include vapors state methods, liquid phase methods (infiltration of preforms, rheocasting/thixoforming, melt stirring and squeeze casting) and solid state methods (powder forming and diffusion bonding). Recently, the preponderance of research studies on Al MMCs has been aimed at developing particle reinforced aluminum matrix composites, based on liquid methods, because they can be used to produce components by casting processes. The fabrication of the composite using casting techniques is particularly attractive since it permits a low-cost and net-shape fabrication,

adaptability of casting processes to existing production practices and flexibility in designing the structure through controlled solidification [1–5]. Discontinuously reinforced metal matrix composites [6] have received much attention because of their improved specific strength and modulus, good wear resistance and modified thermal properties [7]. Composite materials have widened the horizon of engineering materials beyond natural combinations by introducing man-made combinations, even across different categories of materials, metals, ceramics and polymers. The topologically continuous major phase in the composite is called matrix, in which the other minor phase or phases may be discontinuously/continuously distributed to impart/reinforce certain properties. There are many metallic components where wear resistance is the primary consideration for application. Normally, aluminum alloys have excellent mechanical properties coupled with good corrosion resistance but often possess poor resistance to wear and seizure. It is possible to reinforce aluminum alloys by various hard and soft particles such as SiC, Al₂O₃, flyash, glass, WC, graphite, mica, coconut shell char, TiO₂, etc. to impart resistance to wear and seizure [8–10]. Synthesis of aluminum based lightweight composites by economic route of solidification processing [9] has received considerable attention due to significant improvements in the tribological properties of such composites including sliding and abrasive wear resistance, and also, seizure resistance [10–12]. Aluminum based metal matrix composites (AMCs) are promising materials for automotive, aerospace, deep ocean, nuclear energy generation, and other structural applications because of their low density, high stiffness and low wear rate [12, 13]. The wear resistance of the components in the three different materials was ranked. Moreover, analysis of particle distribution and optical and scanning electron microscope observations of reaction products were also performed. Results show that components in aluminum alloy with SiC as reinforcement have a uniform distribution of ceramic particles, sound interface without fragile compounds and wear resistance higher than that of components reinforced with B₄C particles. In recent years, interest in controlling attributes such as coefficient of thermal expansion, thermal conductivity, friction characteristics and wear resistance has arisen. The investigated case study is the production of a pick-holder of a power loom machine. This component is a typical example of a class of products coming from unexplored sectors, which can take advantages of the light weight and high wear resistance of the composite. Indeed, the pick-holder has to be light since during the working of the loom it is moved very fast. Moreover, the surface holding of the pick, which is continually moved up and down, requires high wear resistance. On the contrary, despite its high wear resistance properties, studies dealing with the stir casting method to obtain composite based on B₄C are very scarce. Using the double stir procedure, a variant of the stir casting method, both ceramic carbides are forced to be absorbed by liquid aluminum. Then, the traditional investment casting process, already used to produce the pick-holder in unreinforced aluminum alloy, is extended to obtain the component in composite. Aluminum matrix composites have a wide range of applications where high specific strength and high modulus as well as good wear resistance are the important aspects. Owing to the low density, low melting point, high thermal conductivity of aluminum, a variety of ceramic particulates such as SiC, Al₂O₃, and TiC have been reinforced into it to form the composites. Among these

particulates, titanium diboride, TiB_2 , has emerged as an outstanding reinforcement due to the fact that TiB_2 has high hardness and superior wear resistance, and more importantly, it does not react with aluminum to form any reaction product at the interfaces between the reinforcement and the matrix [14, 15]. Aluminum alloys have been gaining great importance as structural materials, but for many applications it is necessary to improve their wear resistance. In particular, uses of aluminum alloys in automotive applications have been limited due to their inferior strength, rigidity and wear resistance, as compared to those of ferrous alloys. Particle reinforced aluminum composites, nevertheless, offer reduced mass, high stiffness and strength and improved wear resistance. Specifically, the possibility of substituting iron-base materials for Al metal matrix composites (MMCs) in automotive components provides the potential for considerable weight reduction [16]. In this study, the sliding velocity (estimated from the sample rotating speed) and the total sliding distance for all alloys tested were maintained constant at 0.0060 m/s and 16.5 m, respectively. Analysis of the wear tracks was performed using JEOL-JSM 5410 LV and JEOL-JSM 6100 scanning electron microscopes (SEM) equipped with electron dispersive spectroscopy (EDS) capabilities. Back-scattered electron imaging (BEI) was used to analyze the wear track topography and composition in both centrifugally cast and gravity cast composites. This technique was preferred since at low magnification, BEI provides a better view of the surface topography than secondary electron imaging. The wear volume was calculated from topographical analysis of the wear track, using a Nikon SMZ 1500 stereoscope, a Nikon Epiphot 2 optical microscope, and a Nano surf easy Scan TM atomic force microscope (AFM). From this information, the wear coefficient, K , was determined as defined by Eq. (1):

$$K = \frac{W}{F_N S}, \quad (1)$$

where W is the wear volume (mm^3), F_N is the applied load (N), and S is the sliding distance (m) [17].

It has been observed that wear rate increases with increasing normal load but decreases with increasing volume fraction of particles if the bonding between the matrix and the particles is adequate. The main goal of this study is to determine dry sliding wear behavior in the context of formation of transfer layer on the sliding surface of cast Al–5 wt.% Cu composites synthesized by TiO_2 introduced in melt before solidification of the resulting slurry [18].

Experimental Procedures. The liquidus temperature of this alloy was calculated by Pro-Cast software based on chemical composition. By using this software, it is possible to predict the liquidus temperature of aluminum alloys, based on their chemical compositions [19, 20]. Pieces of Al–Si of composition given in Table 1, have been heated in a graphite crucible kept in a vertical electric resistance muffle furnace to attain molten state. When the temperature of the melt reaches $750^\circ C$, melt was mechanically stirred to create a vortex in the melt. Then TiO_2 particles with characteristics described in Table 2 are added into the vortex for their transfer into the melt, and magnesium pieces are also added to the melt to

help wetting of in-situ generated particles by molten aluminum and retain them inside the melt. Melt-particle reaction is allowed to continue for 20 min. To improve the dispersion of the TiO_2 particles in the base metal, mechanical stirring was instituted. This was accomplished by using as a stirrer, a disk of stainless steel, 2 inches in diameter, cut at the radius in 4 or 5 places with the blades bent so that they formed a multi-bladed fan. The stirring unit was mounted at the end of an 18-inch-long, 3/8-inch-diameter rod driven by the stirrer motor operating at 200–1300 rpm. The next step is the addition of TiO_2 particles as the reinforcement. The liquid metal was stirred under a hot argon atmosphere at about 100°C and the maximum flow of $2360 \text{ cm}^3/\text{min}$. Argon was directly injected inside the melt to control the oxidation during the foaming process.

T a b l e 1

Chemical Compositions of Al–Si before and after the Addition of TiO_2

Weight (%)									
Si	Cu	Zn	Fe	Mg	Ti	Mn	Ni	Sn	Pb
6.00	3.50	1.54	0.78	0.15	0.10	0.10	0.02	0.001	0.001

T a b l e 2

Details of Nano TiO_2 Powders Used in Processing of Cast In-Situ Composite

Powder	Purity (%)	ρ , g/m^3	Size	Supplier
Nano TiO_2 (anatase)	99.95	0.4	< 15 nm	Atoor Sanat Abtin Industrial Group, Tehran, Iran.

The resulting slurry of melt containing oxide particles is then cast into a steel mould by bottom pouring. The cast in-situ composite ingot is made to cool very fast by cooling them in water immediately after casting. The Brinell hardness tests of the composites have been carried out with a 2.5 mm diameter hardened steel ball at a load of 31.25 kg to avoid excessive indentation. Molten aluminum was poured in the sand mould with a cylindrical shape of 22 mm in diameter and a length of 350 mm. 2 mm of diameter is to be machined to a standard sample for tensile test according to ASTM-B 577. Tensile test was conducted by the Universal Testing Machine (Gotech) at a strain rate of 10^{-1} s^{-1} at room temperature. Dry sliding wear tests of different cast in-situ composites and un-reinforced alloys have been performed under the ambient condition of relative humidity in the range between 40 and 60% and the temperature between 17 and 25°C , using a pin-on-disk machine, installed in the laboratory of Islamic Azad University of Yazd. The experiments are conducted following ASTM G99-90 standard, using counter face of steel disk 316L/EN-32 hardened to 62–65 HRC. The contact surface of the pin is flat and polished using 1/0, 2/0, 3/0, and 4/0 grade emery papers before conducting the sliding wear test of the pin under five different loads of 10, 20, 30, 40, and 50 N and a fixed sliding speed of 1 m/s [21]. The experimental setup is illustrated in Fig. 1.

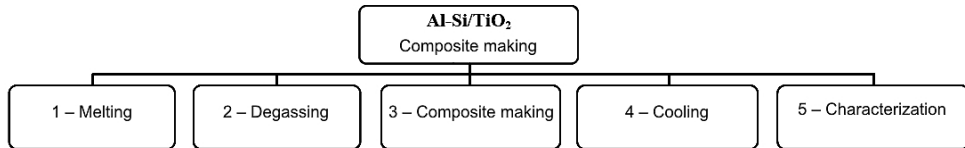


Fig. 1. The experimental set up for ultrasonic treatment of Al-Si TiO₂ composite making.

Results and Discussion. Figure 2 shows the SEM microstructures of composite, as typical examples of composite synthesized by dispersion of TiO₂ in Al-Si alloy. With increasing the addition of oxide particles, there are more bright particles appearing as fine spots, indicated in the microstructure. The bright elongated and faceted precipitates of CuAl₂ are shown in the matrix which is surrounded by TiO₂ particles. Here, with increasing TiO₂ content, the surface becomes rougher (due to an increase in pigment population on the surface) and thus the mechanical interlocking as well as adhesion strength is increased.

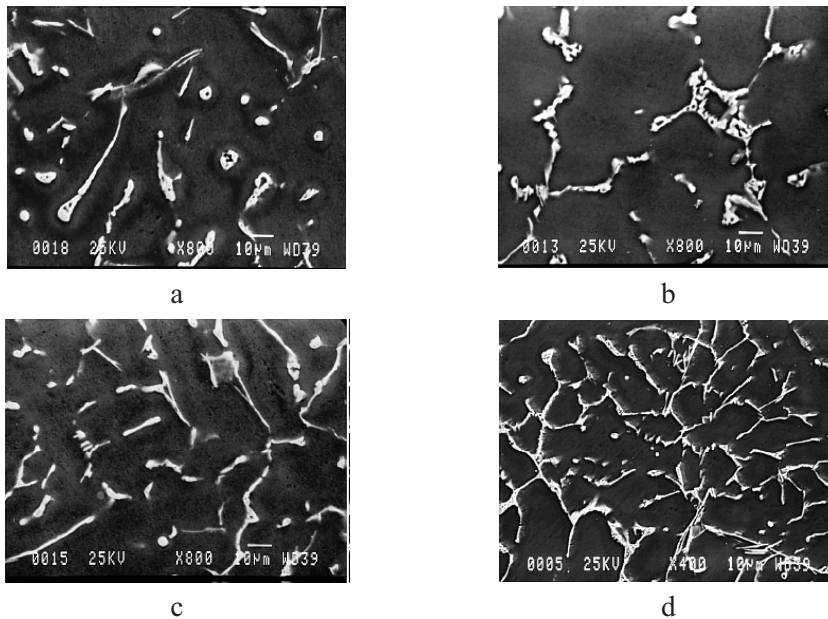


Fig. 2. SEM microstructure of Al-Cu composite with increase in TiO₂ content: (a) 0.5 wt.%; (b) 1.5 wt.%; (c) 2.5 wt.%; (d) 3.5 wt.%.

It can be seen that as the TiO₂ content increases up to 3.5 wt.%, the grain size of the composite material decreases to 10 μm. This decrease in grain size is related to the formation of TiAl₃ phase due to the reaction between Al melt and TiO₂ particles as observed elsewhere [22]. In aluminum alloys, finely dispersed TiAl₃ particles can be derived from the reduction of TiO₂ during thermal processing, which react with the Al matrix to form TiAl₃ in-situ [23]. This phase is formed prior to solidification of Al-Si alloy. Due to its better lattice compatibility with solid aluminum, makes it an efficient nucleation site for aluminum grains upon solidification. The TiAl₃ grains dissolve upon solidification of aluminum and most probably responsible for the enhanced nucleation of aluminum grains [24]. There

are some reinforcement characteristics that influence the mechanical properties of the composites, such as the volume fraction and the shape, size and dispersion of the reinforcement. The strength of Al-TiO₂ composite is strongly dependent on the volume fraction and the particle size of TiO₂. Composites containing larger TiO₂ particle size show increased wear resistance, but reduced tensile strength by comparison with small particle size reinforced composites [25]. Figure 3 shows the variation of hardness with increasing particle content in the composites developed by the addition of TiO₂. The hardness varies more or less linearly with TiO₂ content. The porosity content is shown within bracket. Although in both the systems the hardness varies more or less linearly despite differing porosity content. It can be seen that as the TiO₂ content increases, the hardness of the composite material increases monotonically by significant amounts if other factors are kept constant. Quantitatively, as TiO₂ content is increased from 0.5 to 3.5%. This increase in hardness is due to the fact that TiO₂, being a very hard dispersoid, contributes positively to the hardness of the composite. As is well known, hardness is the resistance to indentation, wherein there will be localized plastic deformation under standardized conditions. The increased hardness is attributable to the hard TiO₂ particles acting as barriers to the movement of dislocations within the matrix.

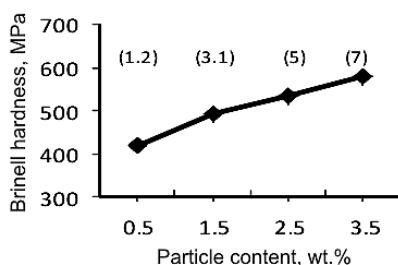


Fig. 3. Variation of hardness of cast composites with increasing TiO₂ particle content.

Figure 4 shows the variation of cumulative volume loss with sliding distance at different normal loads of 10, 20, 30, 40, and 50 N and a fixed sliding speed of 1.0 m/s for different cast in-situ composite designated as 0.5, 1.5, 2.5, and 3.5 wt.% containing the particle and porosity contents of (1.83, 3.45), (1.98, 4.12), (2.4, 5.13), (3.3, 6.88), respectively. The solid lines represent the results of pin-on-disk tests normally carried out, allowing the wear debris to get between the sliding surfaces contributing to three body wear and formation of transfer layer. The dotted lines indicate the results of the tests when the wear debris has been removed continuously by using a camel brush. For a given normal load, the cumulative volume loss increases linearly with increasing sliding distance following Archard's law as commonly observed for metal matrix composites [26] although in dry sliding wear the mechanism is not merely adhesion. Interestingly, the same trend is observed when the wear debris is removed during the test. By comparing Fig. 4a and 4c, it may be observed that the accumulated volume loss increases with increasing particle content. The lines, both solid and dotted, are drawn by linear least square fit and the corresponding load is indicated in the figures. There is no load-induced wear transition in the load range investigated. However, the lines at different normal loads with and without arrangement for the removal of wear

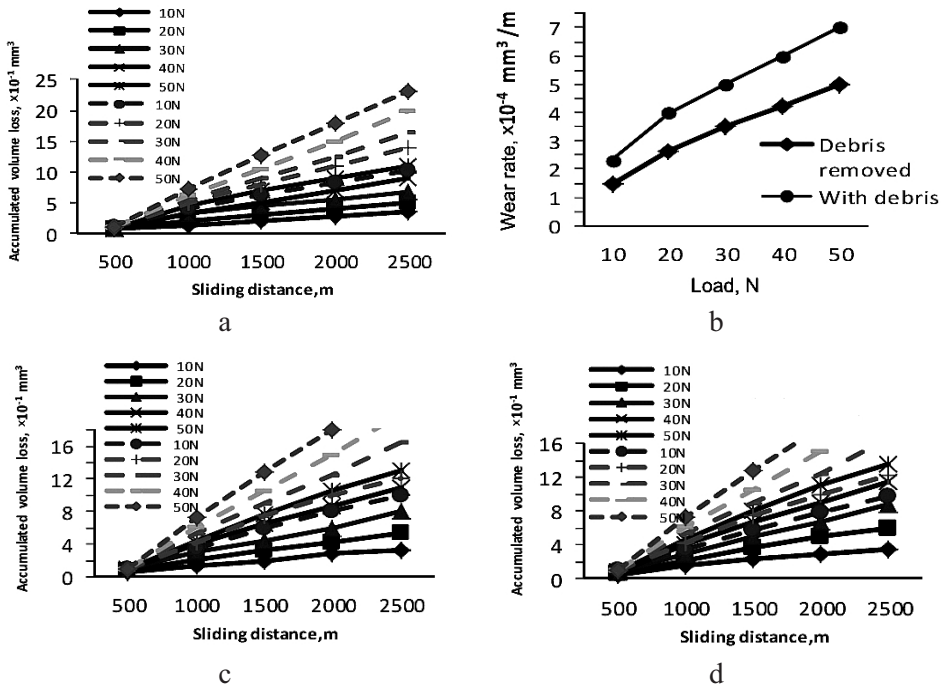


Fig. 4. Variation of accumulated volume loss with sliding distance for the composites designated as (a) 0.5 wt.%, (b) 1.5 wt.%, (c) 2.5 wt.%, and (d) 3.5 wt.% TiO_2 tested at different loads with (dashed line) and without (solid line) removal of wear debris during the test.

debris appear to diverge with increasing sliding distance, and there is significant increase in cumulative volume loss in wear when the wear debris is continuously removed from the wear track.

The variation of wear rate with load in composites (0.5, 1.5, 2.5, and 3.5 wt.% TiO_2) having different particle contents is shown in Fig. 5 for tests with and without removal of wear debris. The wear rates for the composites tested without removal of debris, increase more or less linearly with increasing the load, but their magnitude is relatively close in composites with different particle content. This is because of the difference in particle contents and porosities in composites designated as composites (1.5, 2.5, and 3.5 wt.% TiO_2). The cast composite with a lower particle content as in 0.5 wt.% is generally compensated by a lower porosity. At a given particle content, the wear rate increases with increasing porosity content due to its combined effect on real area of contact and subsurface cracking. The wear rate will be largely controlled by the rate at which particles decohere. On the other hand, when the reinforcing particle are poorly bonded and undergoes decohesion, the contact will be eventually between the matrix and the material counterface and the wear rate of the composite will be comparable or even greater than that of the matrix alloy. The slope of the variation of wear rate with load is less when the wear debris is not removed.

The wear coefficients have been estimated by multiplying the slope of variation of wear rate with load. The wear rate estimated by dividing normal load applied during dry sliding by the hardness of the material. Therefore, a lower real area of contact due to higher hardness may result in a higher wear coefficient

although the wear rates may be similar. Thus, wear coefficient cannot be accepted as a discriminating parameter for wear behavior [27]. The wear coefficient in composites tested without removal of wear debris is between $3.25 \cdot 10^{-6}$ and $4.25 \cdot 10^{-6}$. However, in tests carried out while removing wear debris, it increases to a level between $6 \cdot 10^{-6}$ and $7 \cdot 10^{-6}$ as shown in Fig. 6a. The increase in wear coefficient in tests conducted while removing the debris compared to that observed in tests without removal of debris is a reflection of the enhanced wear rate in the former case as the estimated real area of contact remains the same in a given composite. However, the actual real area of contact may be significantly different because of the dynamic nature of the contact and the formation of transfer layer on the sliding surface in oxidative wear.

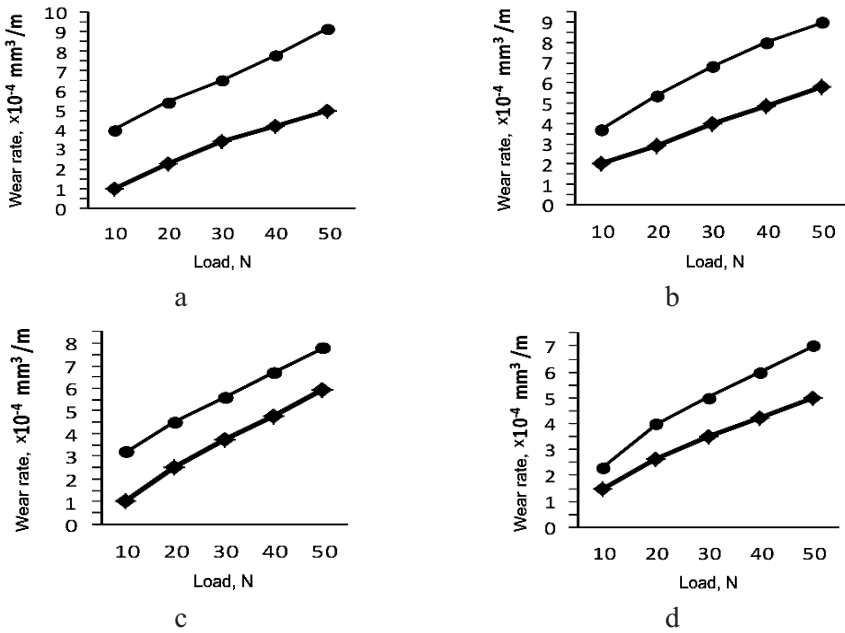


Fig. 5. Variation of wear rate with load or tests carried out with and without removal of wear debris, as observed in the composites designated as (a) 0.5 wt.%, (b) 1.5 wt.%, (c) 2.5 wt.%, and (d) 3.5 wt.% TiO_2 [(◆) debris removed; (●) with debris].

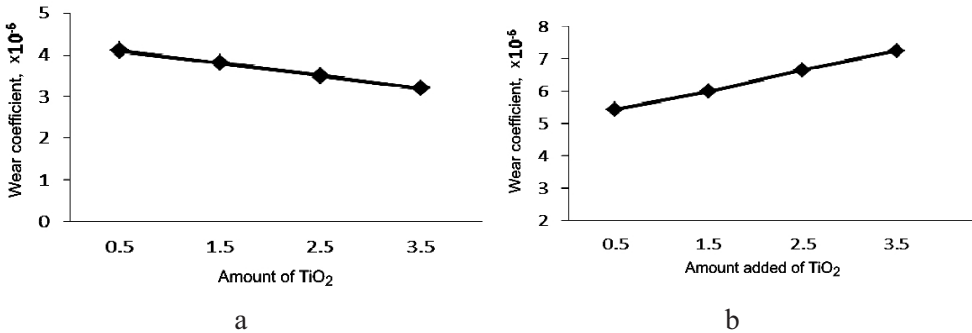


Fig. 6. The variation of wear coefficients with increasing oxide addition in composites developed by addition of TiO_2 (a) while removing debris and (b) without debris removal.

Al–Si alloy and the composites containing oxides have been examined for their friction behavior determined by the variation of coefficient of friction during tests of dry sliding wear under different loads as shown in Fig. 7. The friction force rises in the initial period and then fluctuates around a mean during dry sliding. The mean has been determined from the individual values of coefficient of friction excluding the initial rising part, and it has been observed that the mean coefficient of friction decreases with increasing load for the Al–Si alloy and the composites containing TiO_2 as shown in Fig. 7. At a higher load, the frictional force increases with greater dissipation of energy leading to a higher temperature at contact, which may help better compaction and spread of transfer layer of oxides resulting in lowering of coefficient of friction with increasing load. But higher coefficient of friction with increasing oxide content in the composite is surprising as these particles are supposed to create weak junctions with the asperities of the counter face because of low oxide-metal interfacial energy and also, contribute in the formation of a greater cover of transfer layer which should make relatively weak junctions. Therefore, the only inescapable conclusion is that ploughing of the sliding surface and micro-cutting during three body wears is contributing to higher frictional forces in composites containing more hard oxide particles. However, it may be remembered while interpreting the friction behavior that the coefficient of friction has been fluctuating during dry sliding wear and the trends should be interpreted with caution particularly when the difference between average coefficient of friction is small.

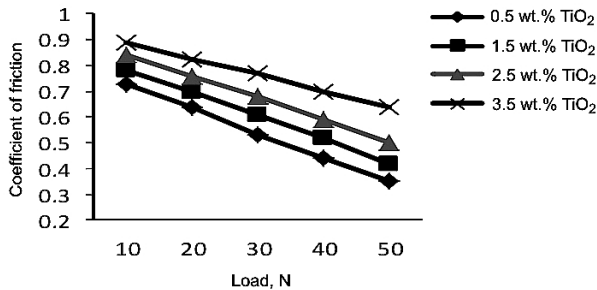


Fig. 7. Coefficient of friction with increasing load in composites developed by addition of TiO_2 along with those of cast commercial aluminum, without debris removal.

The wear debris of composite and cast aluminum have been compared in Fig. 8. Both debris show smaller oxide particles apart from agglomerates which could be flaked off the transfer layer. The agglomerates are relatively smaller for the composites as shown in Fig. 8a, compared to those observed for cast aluminum illustrated in Fig. 8b.

Increase in hardness is expected to decrease the real area of contact. The accumulated loss of volume in dry sliding wear linearly increases with sliding distance in both types of composite developed by the addition of TiO_2 as shown in Fig. 4 for different amounts of oxide addition. It may also be observed that the accumulated volume loss decreases with increasing the particle content. This may be attributed to decreasing the real area of contact during dry sliding due to increasing the hardness of the composites with increasing the particle content. This figure also shows that the accumulated volume loss is considerably higher when

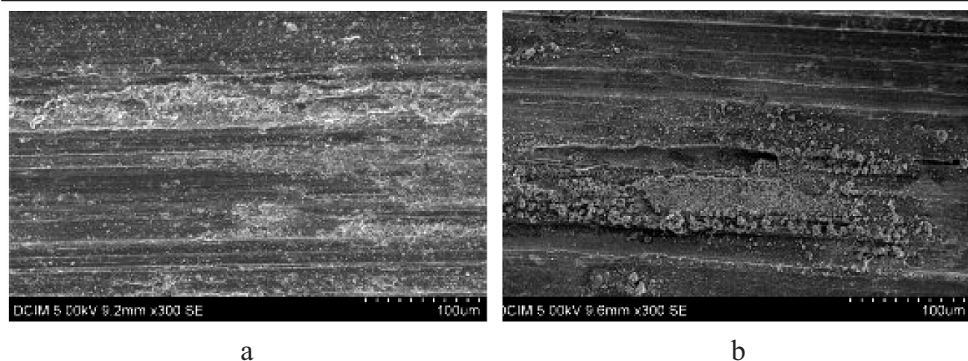


Fig. 8. SEM micrographs of typical samples of wear debris generated during dry sliding of pin samples of (a) Al-Si composite and (b) cast aluminum.

wearing debris is removed during dry sliding wear. Under the conditions used in dry sliding, the wear is primarily oxidative although some metallic chip-like particles are also observed as shown in Fig. 8. The chip-like particles may become generated by ploughing by the asperities of the counter face or by three body wears due to micro-cutting by trapped hard oxides between the sliding surfaces. These hard oxide particles get locked between the sliding surfaces and promote three body wears, which should enhance volume loss in wear. At the same time, these particles get compacted on the sliding surface to form a protective transfer layer, so hard that there are no scoring marks on it. Since the accumulated volume loss in wear is relatively more when the wear debris is removed during dry sliding wear test as shown in Fig. 5, it may be inferred that the beneficial role of wear debris in promoting wear resistance through the formation of transfer layer is more prominent than its contribution to increased volume loss through three body wears. At higher loads, the oxide debris is expected to get better compacted to form transfer layer and spread over a larger area of the sliding surface. However, the volume loss under such circumstances takes place also by flaking of the transfer layer during sliding, apart from the processes of adhesion, micro-cutting and abrasion. At higher loads, the wearing process could be more aggravated by the transfer layer flaking off as indicated by the presence of a chunky sheet of oxide agglomerates in the wear debris as observed in Fig. 8. The present study clearly demonstrates the beneficial role of the transfer layer as evident from the enhanced volume loss in wear and wear rate observed in Figs. 4 and 5, when the debris particles are continuously removed during wear test. It is observed that the higher addition of oxide results in lower accumulated volume loss in wear for the composites developed by the addition of TiO_2 as shown in Fig. 4, and the wear rate also decreases almost linearly with increasing the addition of oxides as shown in Fig. 5. The observed increase in hardness with higher oxide addition is expected to decrease the real area of contact and also, there will be a relatively higher cover of transfer layer. Thus, the higher oxide addition results in decreased wear rate under similar conditions of dry sliding wear. The cover provided by the transfer layer on the sliding surface depends on the load, and it is really surprising that the variation of wear rate with increasing load is still linear in spite of this complication. The lowering of slope with removal of debris may indicate that without the formation

of transfer layer, the variation may have satisfied the limiting behavior of zero wear rates in the limit of load approaching zero. The wear coefficients, which may be considered as wear rate per unit real area of contact, have been estimated for the two types of composites developed by the addition of TiO_2 by multiplying with hardness the slope of variation of wear rate with load. Although the wear rate decreases significantly with increasing the particle content but decreasing the real area of contact in these composites counteracts it to make the wear coefficient relatively insensitive to the increasing of the particle content. The increase in wear coefficient in tests conducted while removing the debris compared to that observed in tests without removal of debris is a reflection of the enhanced wear rate in the former case as the estimated real area of contact remains the same in a given composite. For the manufacturing approach, this composite, besides its normal age-hardenability property, has improved wear resistance. Products made from this Al-Si TiO_2 composite seem to be very suitable for aerospace applications. The composite can be processed to various product forms, for example, sheet, thin plate, thick plate, and extruded or forged products. Products made from this composite can also be used as a cast product, ideally as a die-cast product. Designers and manufacturers, particularly in the aerospace industry, are constantly trying to improve fuel efficiency, product performance and are constantly trying to reduce manufacturing, maintenance and service costs. One way to achieve these goals is by improving the relevant properties of the used aluminum alloys, especially strength and wear resistance, so that a structure made from a particular constituent can be designed more effectively or will have a better overall performance. Further, by improving the relevant material properties for a particular application, the service costs can be significantly reduced by longer inspection intervals of the structure such as an aero plane.

Conclusions

1. The hardness of composites, developed by addition of TiO_2 , increases with increasing the particle content resulting from the increased reaction between the added oxide and the molten alloy during the processing of the composite.
2. During dry sliding against the counter face of the hardened steel disk under conditions of load and sliding speed, the wear is primarily oxidative as evident from wear debris although there also have been some metallic fragments.
3. The accumulated loss of volume in composites linearly increases with sliding distance during both types of tests conducted with and without removal of wear debris. However, in tests conducted while removing wear debris continuously, the accumulated volume loss is significantly more than that in corresponding tests carried out under similar conditions without removal of wear debris. This clearly establishes the beneficial role of the formation of transfer layer, initiated by compaction of the wear debris along the wear track and then spreading around to cover a significant extent of sliding surface, much greater than that observed in cast aluminum.
4. Increasing the addition of oxides, resulting in higher particle content in composites, decreases the accumulated volume loss and the wear rates also decrease almost linearly with increasing the addition of oxides in composites

developed by addition of TiO_2 . This has been attributed to the increased hardness with increasing oxide addition causing a lower true area of contact and also, to a higher amount of oxide available in the debris for the formation of relatively higher covers of transfer layer on the sliding surface.

5. The wear coefficients in composites developed by addition of TiO_2 are relatively insensitive to increasing the particle content since decreasing the true area of contact compensates the effect of decreasing the wear rate.

6. The coefficient of friction in composites increases with increasing the addition of TiO_2 , which has been attributed to the ploughing increase of the sliding surface and micro-cutting during three body wears.

Acknowledgments. The author wishes to express his gratitude to Islamic Azad University Yazd Branch (Grant title: Semisolid Mechanical Alloying of Al-6%Si) for the support of this work.

Резюме

Досліджуваний композит отримано шляхом додання від 0,5 до 3,5 мас.% порошку TiO_2 в алюмінієвий розплав за технологією так званої обробки напівзатвердлого металу, що використовується для отримання алюмінієвих сплавів. Литий композит, отриманий шляхом кристалізації розплаву з частинками TiO_2 у формі, випробовували на знос під час сухого тертя за трибо-схемою диск-шпилька. Випробування проводили без вилучення продуктів зносу згідно зі стандартною схемою і з їх вилученням за допомогою волосяного пензлика. Об'ємний знос композита лінійно зростає зі збільшенням довжини ковзання, а швидкість зносу зростає більш-менш лінійно з підвищенням навантаження. Зі збільшенням вмісту частинок TiO_2 зменшується швидкість зносу під час заданого навантаження. Об'ємний знос композита буде значно вищим, якщо продукти зносу вилучаються в процесі сухого тертя. На електронних мікрографіях зношених контактних поверхонь композитів, отриманих шляхом додання порошку TiO_2 , можна бачити яскраво виражений ущільнений перехідний оксидний шар. За більш високих навантажень оксидні продукти зносу імовірно зменшуються, в результаті чого виникає прошарок, який поширюється на більшу площу поверхні ковзання. Таким чином, вилучення оксидних продуктів зносу зумовлює більший знос композита порівняно з випробуваннями без вилучення.

1. B. Previtali, D. Pucci, and C. Taccardo C, "Application of traditional investment casting process to aluminium matrix composites," *Composites: Part A*, **39**, 1606–1617 (2008).
2. L. Ma, Flores-Vélez, J. Chávez, L. Hernández, and O. Dominguez, "Characterization and properties of aluminum composite materials prepared by powder metallurgy techniques using ceramic solid wastes," *Mater. Manufact. Processes*, **16**, 1–16 (2001).
3. H. Wang, "In-situ Si/Al composite produced by semisolid metal processing," *Mater. Manufact. Processes*, **22**, 696–699 (2007).

4. Ch. W. Wong, M. Gupta, and Lu Li, "Effect of matrix constitution on microstructure and mechanical properties of rheocast metal matrix composites," *Mater. Manufact. Processes*, **13**, 27–52 (1998).
5. M. M. Verdian, "Synthesis of $\text{TiAl}_3\text{-Al}_2\text{O}_3$ composite particles by chemical reactions in molten salts," *Mater. Manufact. Processes*, **25**, 953–955 (2010).
6. J. Hashim, L. Looney, and M. S. J. Hashmi, "Metal matrix composites: production by the stir casting method," *J. Mater. Process. Technol.*, **92-93**, 1–7 (1999).
7. G. Lin, X. U. Hong-yu, Y. U. Kuai, and W. Hong-lin, "Aging behavior of Al_2O_3 short fiber reinforced Al–Cu alloy composites," *Trans. Nonferrous Met. Soc. China*, **17**, 1018–1021 (2007).
8. K. C. Chan and S. H. Chan, "Effect of cell morphology and heat treatment on compressive properties of aluminum foams," *Mater. Manufact. Processes*, **19**, 407–422 (2004).
9. C. S. Ramesh, A. R. Anwar Khan, N. Ravikumar, and P. Savanprabhu, "Prediction of wear coefficient of Al6061– TiO_2 composites," *Wear*, **259**, 602–608 (2005).
10. A. Dey, P. Dey, S. Datta, and A. K. Mukhopadhyay, "A new model for multilayer ceramic composites," *Mater. Manufact. Processes*, **23**, 513–527 (2008).
11. K. M. Shorowordi, A. S. M. A Haseeb, and J. P. Celis, "Velocity effects on the wear, friction and tribochemistry of aluminum MMC sliding against phenolic brake pad," *Wear*, **256**, 1176–1181 (2004).
12. S. K. Chaudhury and S. C. Panigrahi, "Influence of TiO_2 particles on recrystallization kinetics of Al–2Mg– TiO_2 composites," *J. Mater. Process. Technol.*, **182**, 540–548 (2007).
13. L. Krishnamurthy, B. K. Sridhara, and D. Abdul Budan, "Comparative study on the machinability aspects of aluminium silicon carbide and aluminium graphite composites," *Mater. Manufact. Processes*, **22**, 903–908 (2007).
14. P. Poddar, V. C. Srivastava, P. K. De, and K. L. Sahoo, "Processing and mechanical properties of SiC reinforced cast magnesium matrix composites by stir casting process," *Mater. Sci. Eng. A*, **460-461**, 357–364 (2007).
15. Z. Min, W. Gaohui, D. Zuoyong, and J. Longtao, " $\text{TiB}_2\text{P}/\text{Al}$ composite fabricated by squeeze casting technology," *Mater. Sci. Eng. A*, **374**, 303–306 (2004).
16. B. S. Ünlü, "Investigation of tribological and mechanical properties $\text{Al}_2\text{O}_3\text{-SiC}$ reinforced Al composites manufactured by casting or P/M method," *Mater. Design*, **29**, 2002–2008 (2008).
17. Z. Humberto Melgarejo, O. Marcelo Suárez, and Kumar Sridharan, "Microstructure and properties of functionally graded Al–Mg–B composites fabricated by centrifugal casting," *Composites: Part A*, **39**, 1150–1158 (2008).
18. Z. Sarajan and M. Sedigh, "Influences of titanium hydride (TiH_2) content and holding temperature in foamed pure aluminum," *Mater. Manufact. Processes*, **24**, 590–593 (2009).

19. F. C. Robles-Hernandez, M. B. Djurdjevic, W. T. Kierkus, and J. H. Sokolowski, "Calculation of the liquidus temperature for hypo and hypereutectic aluminum silicon alloys," *Mater. Sci. Eng. A*, **396**, 271–276 (2005).
20. S.-N. Chou, J.-L. Huang, D. F. Lii, and H.-H. Lu, "The mechanical properties and microstructure of Al₂O₃/aluminum alloy composites fabricated by squeeze casting," *J. Alloys Comp.*, **436**, 124–130 (2007).
21. A. W. Tesfay, S. K. Nath, and S. Ray, "Effect of transfer layer on dry sliding wear behavior of cast Al-based composites synthesized by addition of TiO₂ and MoO₃," *Wear*, **266**, 1082–1090 (2009).
22. S. K. Chaudhury, C. S. Sivaramakrishnan, and S. C. Panigrahi, "A new spray forming technique for the preparation of aluminum rutile (TiO₂) ex situ particle composite," *J. Mater. Process. Technol.*, **145**, 385–390 (2004).
23. I. C. Barlow, H. Jones, W. M. Rainforth, "Evolution of microstructure and hardening, and the role of Al₃Ti coarsening, during extended thermal treatment in mechanically alloyed Al–Ti–O based materials," *Acta Mater.*, **49**, 1209–1224 (2001).
24. Z. Sarajan, "Nucleation effect of Ti–6Al–4V powder on Al–Si eutectic alloy," *Mater. Manufact. Processes*, **24**, 1354–1358 (2009).
25. G. S. Kataiah and D. P. Girish, *Int. J. Pharm. Stud. Research*, 17–25 (2011).
26. G. R. Li, Y. T. Zhao, H. M. Wang, et al., "Fabrication and properties of in situ (Al₃Zr+Al₂O₃)p/A356 composites cast by permanent mould and squeeze casting," *J. Alloys Comp.*, **471**, 530–535 (2009).
27. R. K. Gautam, S. Ray, S. C. Jain, and S. C. Sharma, "Tribological behaviour of Cu–Cr–SiCp in situ composite," *Wear*, **265**, 902–912 (2008).

Received 25. 09. 2012